

Primljen / Received: 16.4.2015.

Ispravljen / Corrected: 31.7.2015.

Prihvaćen / Accepted: 22.8.2015.

Dostupno online / Available online: 10.1.2016.

Load-bearing capacity of fire exposed composite columns

Authors:



Milivoje Milanović, MSc. CE
State University of Novi Pazar
Faculty of Civil Engineering
milanovicnp@gmail.com



Prof. **Meri Cvetkovska**, PhD. CE
Ss. Cyril and Methodius University in Skopje
Faculty of Civil Engineering
cvetkovska@gf.ukim.edu.mk



Petar Knežević, MSc. CE
State University of Novi Pazar
Faculty of Civil Engineering
petar.knezevic.dunp@gmail.com

Subject review

Milivoje Milanović, Meri Cvetkovska, Petar Knežević

Load-bearing capacity of fire exposed composite columns

The cross-section load-bearing capacity of three types of fire exposed steel-concrete composite columns is analysed in this paper, and the results are compared with the load-bearing capacity of a reference reinforced-concrete column. Mechanical properties of constitutive materials are reduced considerably by high temperatures caused by fire action, which results in a reduced load bearing capacity of columns with regard to the longitudinal force and biaxial bending moment. The reduced load bearing capacity of analysed columns subjected to elevated temperatures is expressed through changes in the M-N interaction curves.

Key words:

composite column, temperature, heat transfer, fire resistance

Pregledni rad

Milivoje Milanović, Meri Cvetkovska, Petar Knežević

Nosivost spregnutih stupova izloženih utjecaju požara

U radu se analizira nosivost poprečnih presjeka triju vrsta spregnutih stupova čelik-beton, a dobiveni rezultati se uspoređuju s nosivošću referentnog armiranobetonskog stupa. Mehanička svojstva sastavnih materijala bitno se pogoršavaju zbog visokih temperatura uzrokovanih djelovanjem požara, što dovodi do smanjenja otpornosti stupa na djelovanje uzdužne sile i dvoosnog momenta savijanja. Smanjenje otpornosti analiziranih stupova pod utjecajem visokih temperatura iskazano je kroz promjenu interakcijskih krivulja M-N.

Ključne riječi:

spregnuti stup, temperatura, provođenje topline, vatrootpornost

Übersichtsarbeit

Milivoje Milanović, Meri Cvetkovska, Petar Knežević

Tragfähigkeit von Verbundstützen unter Brandeinwirkung

In dieser Arbeit wird die Tragfähigkeit der Querschnitte von drei verschiedenen Stützen mit Verbund von Stahl und Beton analysiert. Die Resultate werden der Tragfähigkeit einer als Referenz angenommenen Stahlbetonstütze gegenübergestellt. Mechanische Eigenschaften einzelner Materiale werden bei erhöhter Temperatur aufgrund von Brandeinwirkungen bedeutend beeinträchtigt. Somit werden der Normalkraft- und der zweiachsige Biegezugwiderstand der Stütze abgemindert. Die Reduktion des Widerstandes der untersuchten Stützen bei der Einwirkung hoher Temperaturen wird durch eine Veränderung der M-N Interaktionskurven dargestellt.

Schlüsselwörter:

Verbundstütze, Temperatur, Wärmeleitung, Brandwiderstand

1. Introduction

Nowadays the regulations in many countries require that the structures have to fulfil not only the basic requirements regarding the structures' bearing capacity, stability and serviceability, but also requirements concerning the fire safety of structures, as: the load bearing resistance of the structure can be assumed for a specified time period of fire exposure; the generation and spread of fire and smoke within the building is limited; the spread of fire to neighbouring buildings is limited; the occupants can leave the building or can be rescued by other means; the safety of rescue teams is taken into consideration [1-5].

Generally, fire resistance is the ability of a structure, a part of a structure, or a member, to fulfil its required functions (load bearing function and/or fire separating function) for a specified load level, for a specified fire exposure, and for a specified period of time [1]. Fire behaviour of a member, as well as of the entire structure, depends on many factors, such as: the fire exposure, i.e. the intensity and duration of fire action, the position of elements in relation to fire compartment, i.e. the fire scenario, the structural system and support conditions, the distribution and intensity of the existing loads, the size and shape of elements, as well as the temperature dependence of the thermal and mechanical characteristics of constitutive materials.

Due to the thermal mass of concrete, steel-concrete composite columns have a higher fire resistance than steel columns, and it looks like the composite columns were developed to improve the fire resistance of steel columns [6-13]. In practice, the most often used composite columns are: fully encased steel sections, FES; partially encased steel sections, PES, and concrete filled tubular sections, CFS. The columns with a fully encased steel section may be treated in a way similar to the treatment of reinforced concrete columns. Concrete covers the steel section and protects it from intensive heating, i.e. it acts like the steel section insulator. In case of partially encased steel sections, the flanges of the steel section are directly exposed to fire, and the "heat shield" effect of concrete is reduced. In case of concrete filled tubular sections, the steel section is directly exposed to high temperatures, while the concrete core remains cold and behaves like a "heat sink". In such cases, stresses are redistributed to the relatively cool concrete core and the fire resistance is much higher than in the case of steel columns devoid of concrete core.

The load-bearing capacity of the column cross section can be determined from the "bending moment-axial force" interaction curve. At elevated temperatures, the stress-strain characteristics of concrete and steel become non-linear and deteriorate rapidly [4]. This effect directly causes reduction of the axial force and bending moment that can be assumed by the column cross section. The interaction curve of the column cross section is also reduced.

Over the past twenty years, many different design methods have been used for producing the M-N interaction diagrams for reinforced concrete and steel-concrete composite columns

at high temperatures. When referring to short columns, whose length has no influence on the bearing capacity of columns, methods suggested by Chen et. al. [13] and Cvetkovska [14] should be mentioned. These methods are based on material nonlinearity only, while the geometrical nonlinearity is neglected. Internal forces are integrated in each time step on the basis of the previously defined temperature field in the column cross section, taking also into account the Navier's hypothesis and the temperature dependent constitutive laws for steel and concrete.

When referring to slender columns, the second order effects should be taken into account. Results obtained by numerical procedures based on this approach are closer to experimental results. Although there are ample data in literature on the temperature dependent interaction curves for concrete filled tubular sections [10, 11] and fully encased steel sections [12], there are no data on the comparative analysis of temperature dependent interaction curves for different types of steel-concrete composite sections. The purpose of the analysis presented in this paper is to define which type of cross section is more suitable from the aspect of higher fire resistance. Therefore, four different types of columns are analysed, three of which are steel concrete composite columns with different cross sections (fully encased steel sections FES, partially encased steel sections PES, and concrete filled tubular sections CFS), while the fourth one is a reinforced concrete column adopted for comparison purposes, so as to draw necessary conclusions regarding the advantage of steel concrete composite columns over the reinforced concrete columns of the same size and the same initial loads. The "bending moment-axial force" interaction curves for all four types of columns are produced as a function of the time period of standard fire exposure, and conclusions are made about fire resistance of the columns. The computer program SAFIR [15] (developed by J. M. Franssen at the University of Liege in Belgium), is used for that purpose. The procedure for producing the temperature dependent M-N interaction diagrams of composite columns is based on the simplified method recommended in Eurocode 4, Part 1-2 [4].

2. M-N interaction curve for composite column cross section

In case when the axial force and the bending moment act simultaneously on the column cross section, the load-bearing capacity of the column can be defined from the "bending moment-axial force" interaction curve, which presents the relationship between the design value of plastic resistance to axial compression of the total cross-section $N_{pl,Rd}$, and the design value of the bending moment resistance $M_{pl,Rd}$. Figure 1 [3-5]. The plastic resistance to compression $N_{pl,Rd}$ of a composite cross-section should be calculated by adding plastic resistances of its components:

$$N_{pl,Rd} = A_a \cdot f_{yd} + 0,85 A_c \cdot f_{cd} + A_s \cdot f_{sd} \quad (1)$$

where:

A_a, A_s i A_c - are cross-sectional areas of the structural steel section, reinforcement and concrete

f_{yd}, f_{sd} i f_{cd} - are design values of the yield strength of structural steel, yield strength of reinforcing steel, and the compressive strength of concrete cylinder.

Equation (1) is used for the totally encased and partially encased steel sections. For concrete filled sections the coefficient 0.85 may be replaced with 1.0. The simplified M-N interaction curve is defined with 4 characteristic points: A, B, C and D (Figure 1).

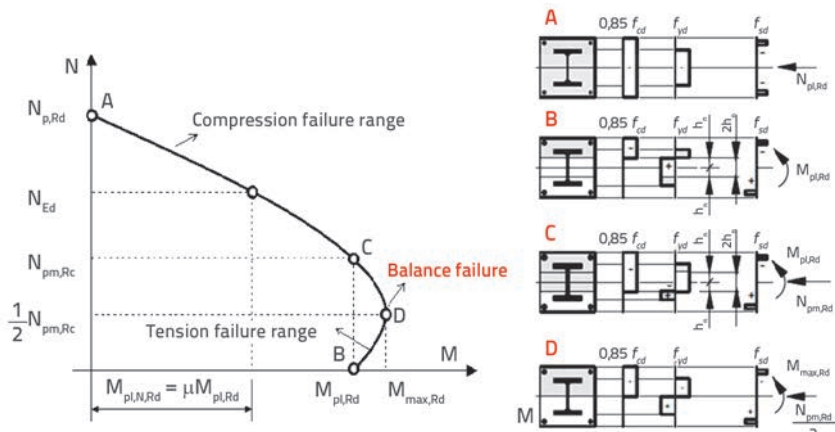


Figure 1. Simplified interaction curve for composite column and corresponding stress distribution

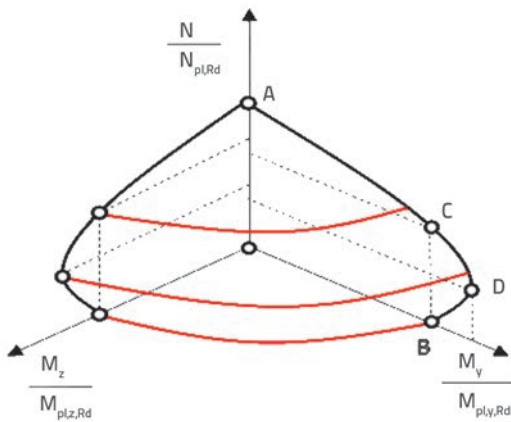


Figure 2. M-N interaction curve for biaxial bending moments

Point A is defined with the design plastic resistance of composite section to compressive normal force $N_{pl,Rd}$ while the bending moment is zero (eccentricity $e=0$).

Point B is defined with the design plastic resistance moment of composite section $M_{pl,Rd}$ while the axial force is zero (eccentricity $e=\infty$).

Point C is defined with the design resistance of concrete to compressive normal force $N_{pm,Rd} = 0.85 A_c f_{cd}$ (for fully or partially encased steel sections) or $N_{pm,Rd} = A_c f_{cd}$ (for concrete filled tubular steel sections), while the bending moment is equal to $M_{pl,Rd}$.

Point D is defined with the maximum design resistance moment $M_{max,Rd}$ in the presence of a compressive normal force $0.5 N_{pm,Rd}$. The design value of the compressive normal force N_{Ed} corresponds to the design value of the plastic resistance moment of the composite section taking into account the compressive normal force $M_{pl,N,Rd}$.

In case when the cross section is exposed to axial force and bending moments about both axes (weak and strong), the load-bearing capacity of the column is graphically presented with the combination of two interaction curves for each axis, respectively, Figure 2.

3. M-N interaction curve for composite column cross section in fire situation

The stress-strain characteristics of concrete and steel become non-linear at elevated temperatures and deteriorate rapidly [2, 4]. This effect directly reflects on the reduction of the axial force and the bending moment that can be assumed by the columns. Interaction curves of the columns cross sections are also reduced. Production of the M-N interaction curves for the defined fire model and defined fire exposure time is only possible if the temperature distribution in the cross section of the column is known.

One of the options for solving this problem is the Finite Element Method (FEM). In this case, the column has to be discretized into a number of elements and the cross section of the column has to be discretized into a number of smaller segments, i.e. sub-slices. The same finite element mesh has to be used for the nonlinear and transient thermal analysis, and for production of the M-N interaction curves [14, 15].

3.1. Numerical procedure for nonlinear and transient thermal analysis

The thermal analysis is an essential component for calculating fire resistance because the load capacity of a structural member/assembly depends on its internal temperature. When a column is exposed to fire, a temperature gradient occurs within the column. The temperature distribution in the cross section of the elements exposed to fire can be calculated using the Theory of Heat Transfer. The governing differential equation for the conductive heat transfer is [14]:

$$\frac{\partial}{\partial x}(\lambda_x \frac{\partial T}{\partial x}) + \frac{\partial}{\partial y}(\lambda_y \frac{\partial T}{\partial y}) + \frac{\partial}{\partial z}(\lambda_z \frac{\partial T}{\partial z}) = \rho c \frac{\partial T}{\partial t} \quad (2)$$

where:

λ - is the thermal conductivity (temperature dependent)

ρ - is the density of material (temperature dependent)

c - is the specific heat (temperature dependent).

Fire boundary conditions can be modelled in terms of both convective and radiative heat transfer mechanisms. The heat flow caused by convection is:

$$q_c = h_c(T_m - T_f) \tag{3}$$

where:

h_c - is the coefficient of convection (for surface exposed to fire $h_c = 25 \text{ W/m}^2 \text{ K}$, and for an unexposed surface $h_c = 9 \text{ W/m}^2 \text{ K}$). These values are recommended in Eurocode 1-1-2 [1]

T_m - is the temperature at the boundary of the element

T_f - is the temperature of fluid around the element.

The heat flow caused by radiation is:

$$q_r = \Phi \varepsilon \sigma_c (T_{m,a}^4 - T_{f,a}^4) = h_r (T_m - T_f) \tag{4}$$

$$h_r = \Phi \varepsilon \sigma_c (T_{m,a}^2 + T_{f,a}^2) (T_{m,a} - T_{f,a}) \tag{5}$$

where:

h_r - is the coefficient of radiation (temperature dependant)

Φ - is the radiation view factor (recommended: $V = 0$)

ε - is the resultant coefficient of emission $\varepsilon = \varepsilon_f \varepsilon_m$;

ε_f - is the coefficient of emission for the fire compartment (zone in which the fire reserves)

ε_m - is the coefficient of emission for the surface of the element

σ_c - is the Stefan-Boltzmann constant

$T_{m,a}$ - is the absolute temperature of the surface

$T_{f,a}$ - is the absolute gas temperature.

Using a typical Galerkin finite element approach, Equation (2) assumes the form:

$$\int_V N^T \left[\lambda_x \frac{\partial^2 T}{\partial x^2} + \lambda_y \frac{\partial^2 T}{\partial y^2} + \lambda_z \frac{\partial^2 T}{\partial z^2} - \rho c \frac{\partial T}{\partial t} \right] dV = 0 \tag{6}$$

where the approximation field function is expressed in terms of the interpolation function as:

$$T = N \cdot T_e \tag{7}$$

The problem is completely solved through equation (6), by applying initial and boundary conditions.

The presented heat transfer equation is a part of the computer program SAFIR [15] that was used in this study. The program is based on the finite element method and the following assumptions are made: fire can be modelled by a single valued gas temperature history; ISO 834 or other fire model; no contact resistance to heat transmission occurs at the interface between the reinforcing steel and concrete; fire boundary conditions can be modelled in terms of both convective and radiating heat transfer mechanisms; temperature dependant material

properties are known and are recommended in Eurocode 4, Part 1.2 [4]; while cracks appear, or some parts of the element crush, heat penetrates in the cross section easier, which is neglected in this study. It is assumed that the changes in the element internal energy, caused by changes in the temperature field of the element cross section, do not influence the work of the internal forces and in each time step the heat flow analysis is separable and parallel with the structural analysis.

3.2. Numerical procedure for defining the M-N interaction curves in fire situation

Once the cross section of the column is discretized into a number of finite elements or sub-slices, (Figure 3), and after the time dependent temperature field is defined, the corresponding curvature φ for plastic resistance of the cross section, and the number of steps for increasing the curvature up to the maximum φ , are assigned.

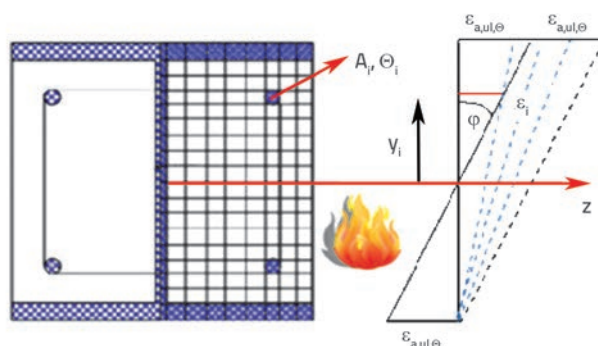


Figure 3. Discretization of column cross section into sub-slices, and corresponding strains of elements for the strong axis "z"

Free strains are determined for each sub-slice at the beginning of a time step, and they do not vary during iteration within a time step. For the concrete or steel sub-slice, they are calculated according to the following equations:

$$\varepsilon_i^{f,c} = \varepsilon_{i-1}^{f,c} + \Delta \varepsilon_i^{cr,c} + \Delta \varepsilon_i^{tr,c} + \Delta \varepsilon_i^{th,c} \tag{8}$$

$$\varepsilon_i^{f,a} = \varepsilon_{i-1}^{f,a} + \Delta \varepsilon_i^{cr,a} + \Delta \varepsilon_i^{th,a} \tag{9}$$

where:

ε_i^f - free strain of concrete, or steel sub-slice, for time step i

$\Delta \varepsilon_i^c$ - free creep strain, accumulated over current time step i

$\Delta \varepsilon_i^{tr,c}$ - transient strain, accumulated only in concrete sub-slice over current time step i

$\Delta \varepsilon_i^{th}$ - free thermal expansion, accumulated over current time step i.

It is assumed that there is a deformational compatibility between steel and concrete at contact surfaces. The " $\sigma - \varepsilon$ " relations, recommended by Eurocode 4, Part 1.2, take into account the creep of concrete and steel at elevated

temperatures. This is done by moving the maxima in the stress-strain curves to higher strains with higher temperatures. When compressed concrete is heated for the first time, the total strain differs from the total strain measured during the constant temperature creep tests, and an additional irrecoverable "transient strain" must be taken into account. This transient strain is a function of the level of stress and thermal expansion [16]. The increment of transient strain at any given time step can be computed as:

$$\Delta \varepsilon_i^{tr,c} = -2.35 \frac{\sigma_{ic}(\theta)}{f_{c,20^\circ C}} \Delta \varepsilon_i^{th,c} \quad (10)$$

where:

- $\Delta \varepsilon_i^{tr,c}$ - transient strain, accumulated over the current time step "i"
- $\Delta \varepsilon_i^{th,c}$ - free thermal expansion accumulated over the current time step "i"
- $\sigma_{ic}(\theta)$ - compressive stress at the corresponding temperature of the sub-slice
- $f_{c,20^\circ C}$ - compressive strength of concrete at ambient conditions (20°).

If the transient strain is not included in structural analysis, the result is a stiffer structural model at elevated temperatures, when computed thermal stresses become very large and failure is predicted to occur much earlier than experimentally observed [14, 16].

The corresponding stresses $\sigma(\theta)$ are defined from the "σ - ε" curves depending on the temperature and appropriate strains of the elements "i". The temperature dependent "s-e" curves for steel and concrete are given in Eurocode 4, Part 1-2 [4].

Once the stresses $\sigma(\theta)$ are defined, the equations (11), (12) and (13) define the axial force and the bending moment about the strong axis "z" and weak axis "y" for the current temperature distribution of the composite column cross section.

$$N = \int_A \sigma(\theta) dA = \int_{y,z} \sigma(\theta) dydz = \sum \sigma(\theta_i) \Delta y_i \Delta z_i \quad (11)$$

$$M_z = \int_A \sigma(\theta) y dA = \int_{y,z} \sigma(\theta) y dydz = \sum \sigma(\theta_i) y_i \Delta y_i \Delta z_i \quad (12)$$

$$M_y = \int_A \sigma(\theta) z dA = \int_{y,z} \sigma(\theta) z dydz = \sum \sigma(\theta_i) z_i \Delta y_i \Delta z_i \quad (13)$$

According to Eurocode 4 Part 1-2, the simplified procedure for the construction of M-N interaction curves of composite columns at ambient temperatures can be used even for fire exposed columns. In this case, the design value of plastic resistance to axial compression is given by:

$$N_{fi,pl,Rd} = \sum_j (A_{s,j} f_{sy,j}) / \gamma_{M,fi,s} + \sum_k (A_{s,k} f_{sy,k}) / \gamma_{M,fi,s} + \sum_m (A_{c,m} f_{c,m}) / \gamma_{M,fi,c} \quad (14)$$

where:

- $A_{i,\theta}$ - is the area of each element (of the cross-section with defined temperature θ)
- $f_{s,\theta}$ - is the effective yield strength of structural steel at temperature θ
- $f_{sy,\theta}$ - is the effective yield strength of reinforcing steel at temperature θ
- $f_{c,\theta}$ - is the characteristic value of concrete-cylinder compressive strength at temperature θ
- $\gamma_{M,fi,a}$ - is the partial factor for the structural steel strength in the fire situation
- $\gamma_{M,fi,c}$ - is the partial factor for the strength of concrete in the fire situation
- $\gamma_{M,fi,s}$ - is the partial factor for the strength of reinforcing bars in the fire situation.

For mechanical properties of steel and concrete, the recommended values of partial factors for the fire situation are: $\gamma_{M,fi,a} = \gamma_{M,fi,c} = \gamma_{M,fi,s} = 1,0$.

3.3. M-N interaction curves of different types of composite columns in fire situation

The above described procedure is a part of the computer program SAFIR [15]. This program was used to define temperature fields in four different types of cross sections (Figure 4) exposed to ISO 834 standard fire from all four sides, and only the heating phase was treated. Cross sections of composite columns are: PES – partially encased steel profile HE 300A with an additional 4Ø18 reinforcement; CFS – concrete filled tubular section with an additional 4Ø18 reinforcement, FES – fully encased steel section HE 260A profile; and RC - reinforced concrete section 40

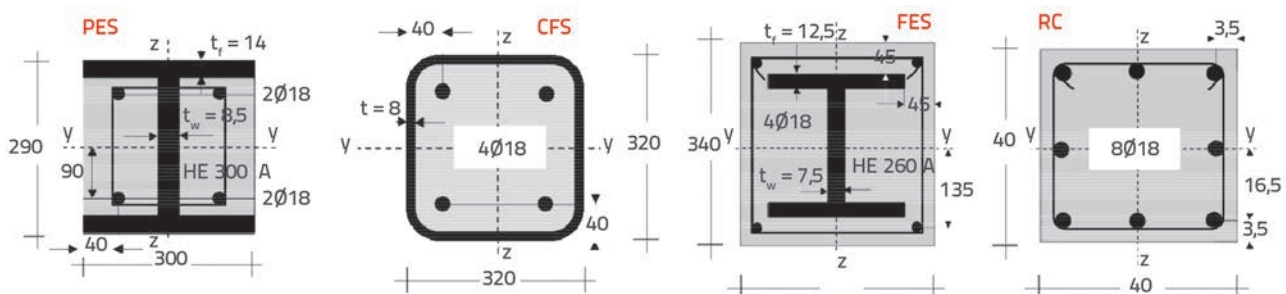


Figure 4. Cross section geometry of columns: PES – partially encased steel profile; CFS – concrete filled hollow section; FES – fully encased steel section; and RC - reinforced concrete section

x 40 cm, reinforced with 8Ø25, for comparison. In this case, the RC section was treated as a composite section and the simplified procedure for M-N diagrams, recommended in Eurocode 4 Part 1-2, was used. The criterion for dimensioning the columns was the design value of plastic resistance to axial compression, and this value is close to 5500 kN for all four cross sections (Table 2). From the aspect of heat transfer and temperature distribution in the cross section of the columns, the dimensions of the three types of composite sections are almost the same, while only the RC cross section exhibits bigger dimensions. Thermal and mechanical properties of steel, concrete and reinforcement

were adopted according to recommendations given in Eurocode 4, Part 1-2, as shown in Table 1. Temperature-dependent specific heat of concrete is defined in Eurocode 4, Part 1-2, and depends on the humidity of concrete. In this analysis, the humidity of concrete was assumed to be 2 %. The number of finite elements (sub-slices) used for discretization of cross sections, as well as the design value of plastic resistance to axial compression for all four columns, are presented in Table 2. Time dependent temperature fields of the analysed cross sections, obtained by SAFIR software, are presented in Figures 5-8.

Table 1. Thermal and mechanical properties of materials used in column cross sections

Thermal and mechanical properties	Steel S355	Concrete C30/37	Reinforcement RA400/500
Convective heat transfer coefficient for fire exposed surface [W/m²K]	25	25	-
Convective heat transfer coefficient for unexposed surface [W/m²K]	9	9	-
Thermal conductivity [W/mK]	45	1,6	45
Emissivity coefficient	0,9	0,8	-
Humidity [%]	-	2	-
Yield strength of steel [MPa]	355		
Yield strength of reinforcement [MPa]			400
Compressive strength of concrete [MPa]		30	

Table 2. Number of finite elements used for discretization of column cross sections, and design values of plastic resistance to axial compression at ambient temperature

Type of cross section	Number of finite elements	N _{pl,Rd} [kN]
PES – partially encased steel profile	3348	5617
CFS – concrete filled hollow section	3446	5529
FES – fully encased steel section	3326	5383
RC - reinforced concrete section	3488	5122

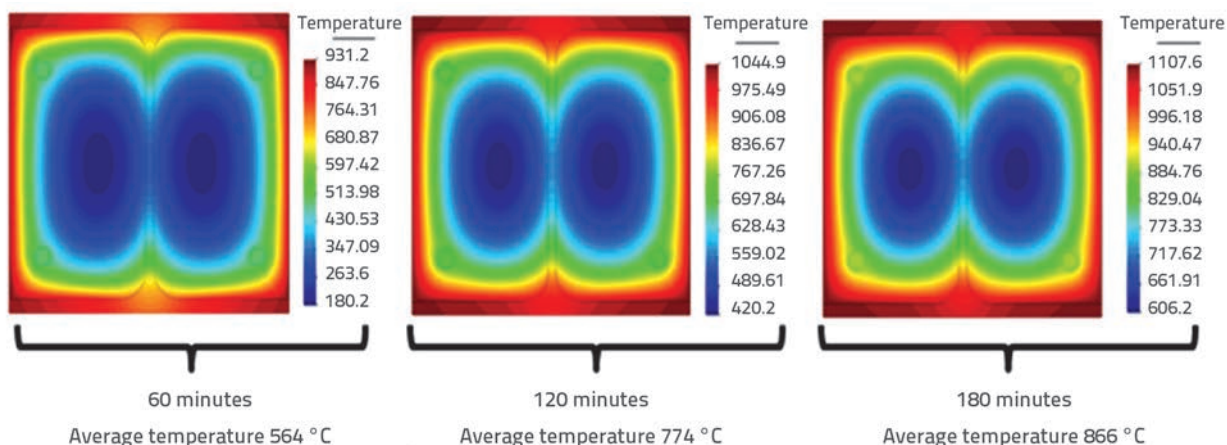


Figure 5. Time dependent temperature field of partially encased steel section (PES)

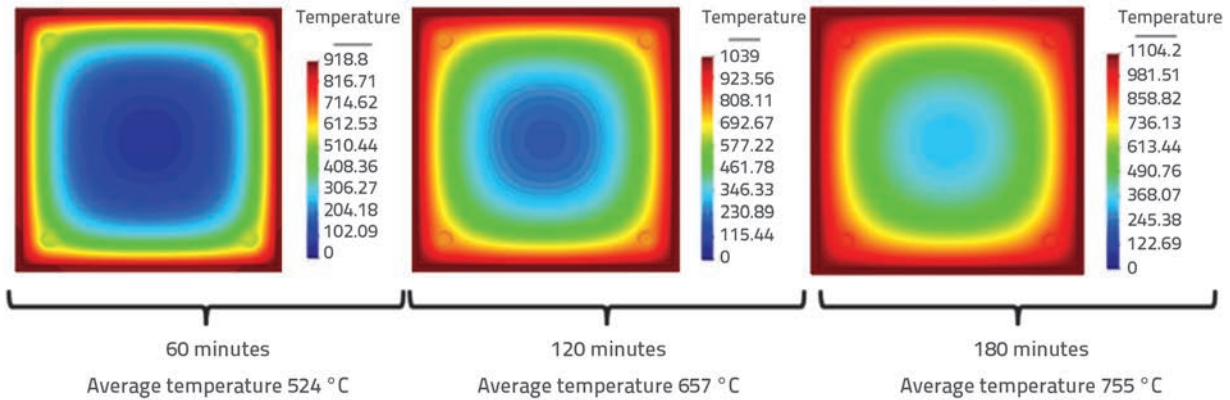


Figure 6. Time dependent temperature field of concrete filled tubular section (CFS)

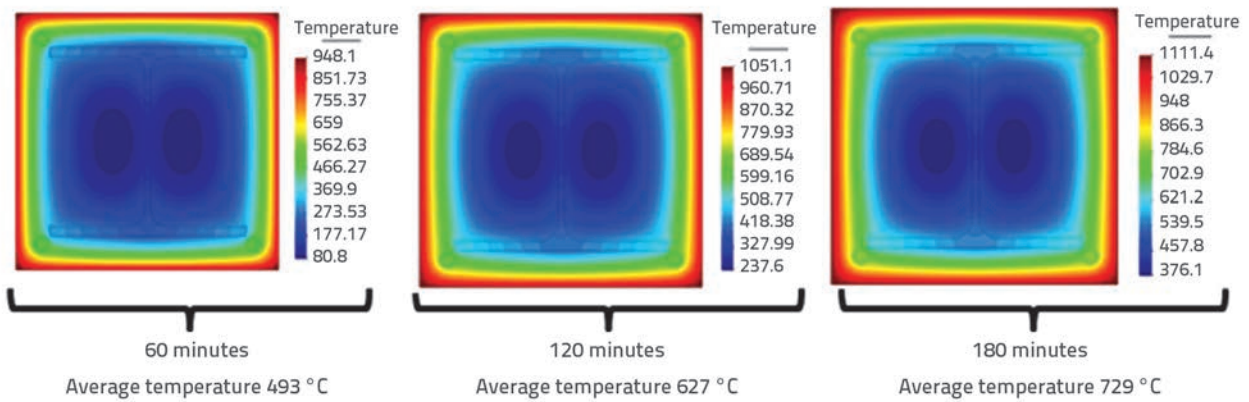


Figure 7. Time dependent temperature field of fully encased steel section (FES)

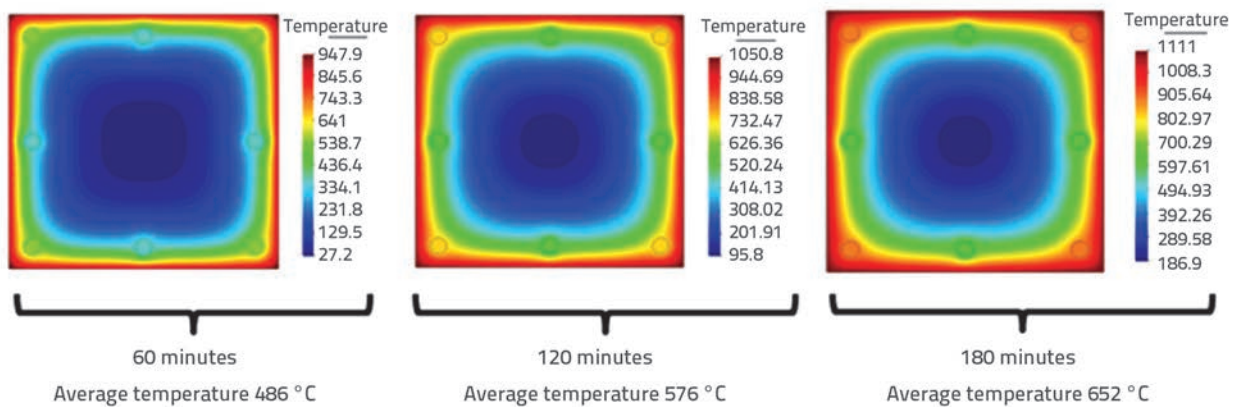


Figure 8. Time dependent temperature field of reinforced concrete cross section (RC)

The "bending moment-axial force" interaction curves for all four types of columns were produced as a function of the time period of standard fire exposure according to the simplified procedure recommended in EN 1994-1-2, as shown in Figures 9-11. The curves are different in case of bending moment about

the strong axis and about the weak axis. High temperatures caused by fire action considerably reduce mechanical properties of constitutive materials. Consequently, the axial force and the biaxial bending moment bearing capacities of the columns are reduced, resulting in changes to the M-N interaction diagrams.

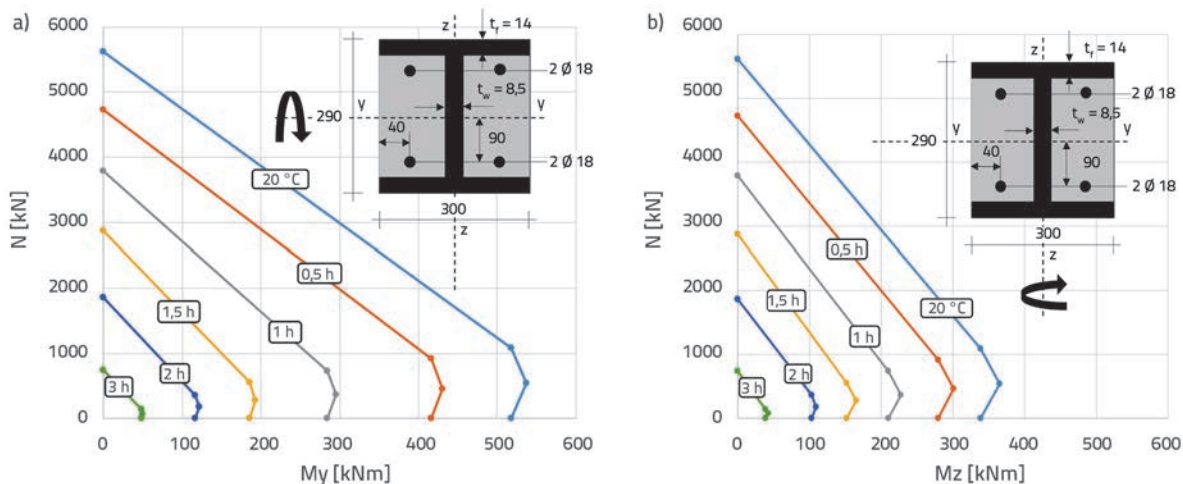


Figure 9. M-N Interaction curves for bending moments about the strong and weak axes of the PES - partially encased steel section, at different moments of fire exposure

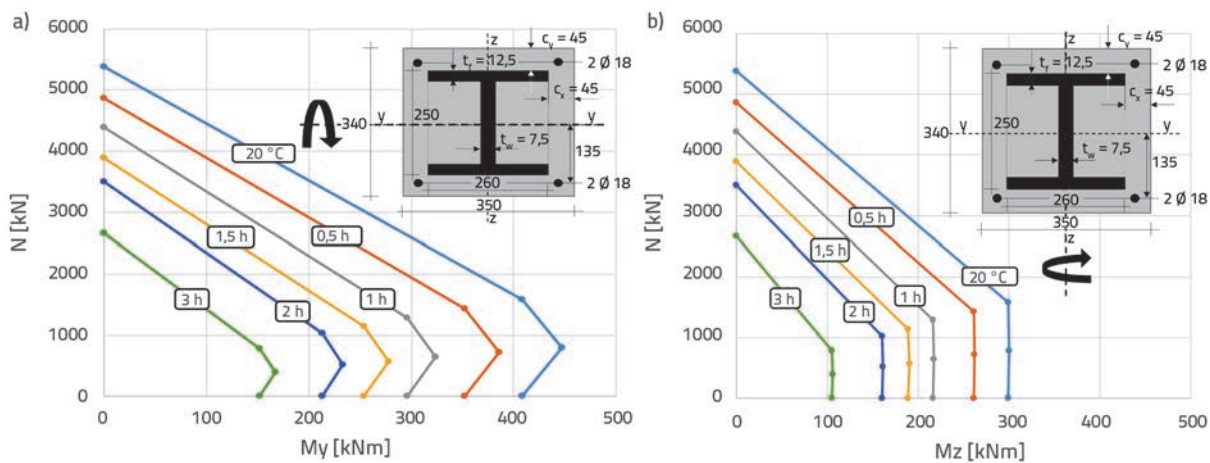


Figure 10. M-N Interaction curves for bending moments about the strong and weak axes of the FES - fully encased steel section, at different moments of fire exposure

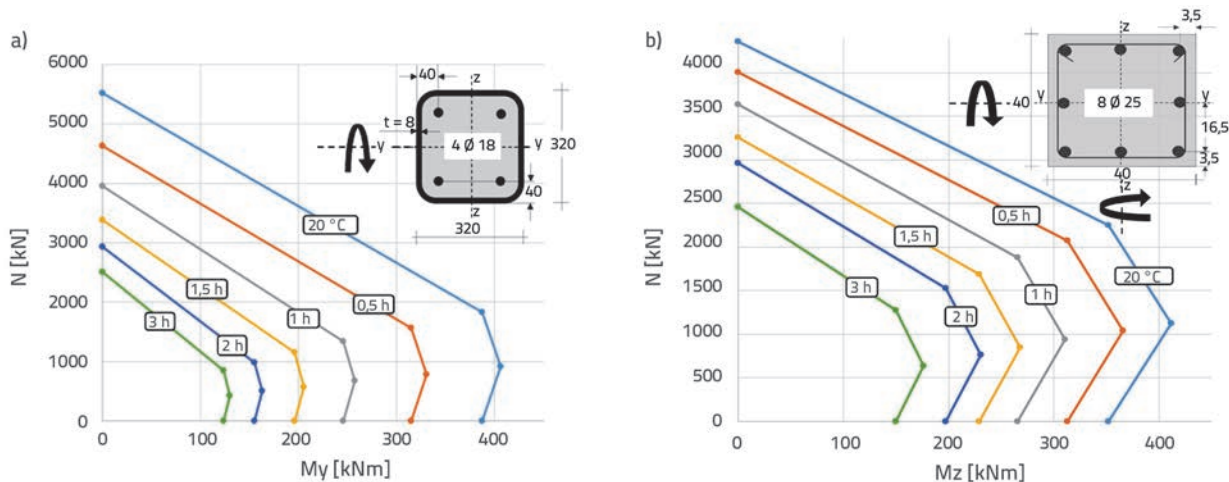


Figure 11. M-N Interaction curves of: a) CFS-concrete filled hollow section, b) reinforced concrete cross section, at different moments of fire exposure (RC)

The presented numerical procedure for producing the M-N interaction diagrams depends on the discretization of cross section. Therefore, the convergence study on the number of finite elements in the cross section of the CFS (concrete filled hollow section) was conducted, and the results for two characteristic moments ($t=1$ hour and $t=2$ hours) are presented in Figure 12. The calculation performed with 3446 finite elements is assumed to be the reference one and, in case of 2006 finite elements, the bending moment values for points B, C, and D are by 1 % lower, while in case of 1006 finite elements the values are 4 % lower compared to the reference value. Differences in the axial force values are found only for points A, and they amount to 1 % in case of 2006 elements, and 4 % in case of 1006 elements. In order to improve the results, all further calculations were conducted with more than 3300 finite elements.

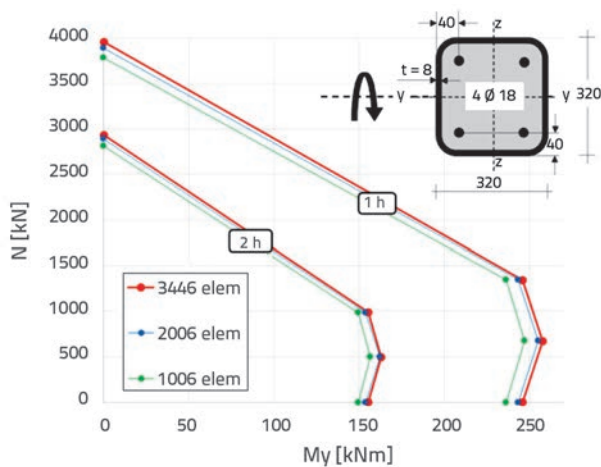


Figure 12. Comparison of M-N Interaction curves for concrete filled hollow section (CFS) at characteristic moments of fire exposure, defined with different numbers of finite elements

The above figure shows a significant reduction in bearing capacity of the analysed cross section types, caused by high temperatures during fire action. However, the loss of bearing capacity in cross section is not the same for all types of composite sections [17-20]. At ambient temperature, for the same dimensions of cross section, the partially encased steel sections have the highest ultimate strength because the steel profile participates with a high percentage in the total area of cross section. For these four types of cross section, the reinforced concrete section has the lowest initial bearing capacity, with reinforcement taking up 1 % of the section.

In case of fire, the fully encased section (Figure 10) has the highest fire resistance, while the partially encased section and the concrete filled hollow section exhibit lower fire resistance (Figures 9 and 11a). Steel profiles significantly increase the initial bearing capacity of partially encased sections and the concrete filled hollow sections but, because of the peripheral position of steel, it heats to high temperatures in a relatively

short time period, and mechanical properties of steel are reduced, which results in a lower fire resistance. The steel profile of the totally encased section is situated in the interior of the section, and it is protected by concrete that has a low thermal conductivity, and so the steel stays cooler for a longer period of time and keeps its mechanical properties, thus providing a higher fire resistance. An additional disadvantage of the partially encased section, in terms of fire resistance, is the proportional participation of the steel section which is higher than the one in the concrete filled hollow section; therefore, the partially encased section has a higher ultimate strength for service conditions [19, 20].

When assessing the loss of bearing capacity at cross section, it is important to take into account the value of the average temperature of cross section, as related to the corresponding time of fire exposure. The average temperature of cross section was calculated by summarizing temperatures in each sub-slice, and the sum was divided with the total number of sub-slices. Figure 13.a presents average cross-section temperatures for four different types of columns that are analysed in this study. The reinforced concrete column reaches the lowest average temperature in cross section. There are two reasons for that: the cross-section dimensions are bigger compared to other columns, and the coefficient of thermal conductivity of concrete is much lower than that of steel. In case of the partially encased steel section, the steel-section flanges are directly exposed to fire, the effect of concrete as a "heat shield" is less pronounced, and so this type of cross section reaches the highest average temperature. In case of concrete filled tubular sections, the steel section is directly exposed to high temperatures while the concrete core remains cold and behaves as a "heat sink".

Three different stages of the average column cross section temperatures can be defined. The first stage refers to temperatures after 30 minutes of heating. These temperatures are almost identical, which can be explained by the short heating period, and the inability of temperature to penetrate deeper into the section. The second stage represents the heating period ranging from 30 to 120 minutes. It is characterized not only by a general rise in temperature in all cross sections, but also by considerable differences in average temperatures. During the third stage, the differences in average temperatures for the FES and CFS cross sections begins to decrease with an increase in heating time (over 120 minutes). The FES section temperature tends to increase almost linearly. The concrete part of the CFS section opposes the temperature penetration into the cross section, and this effect results in a slow increase in the average temperature. The same effect is observed for the RC section. In the PES section, the position and direct exposure of the steel element result in a continuous increase in the average temperature.

The changes in average cross-section temperatures during the heating period are crucial for the analysis and better understanding of the M-N interaction curves of the columns.

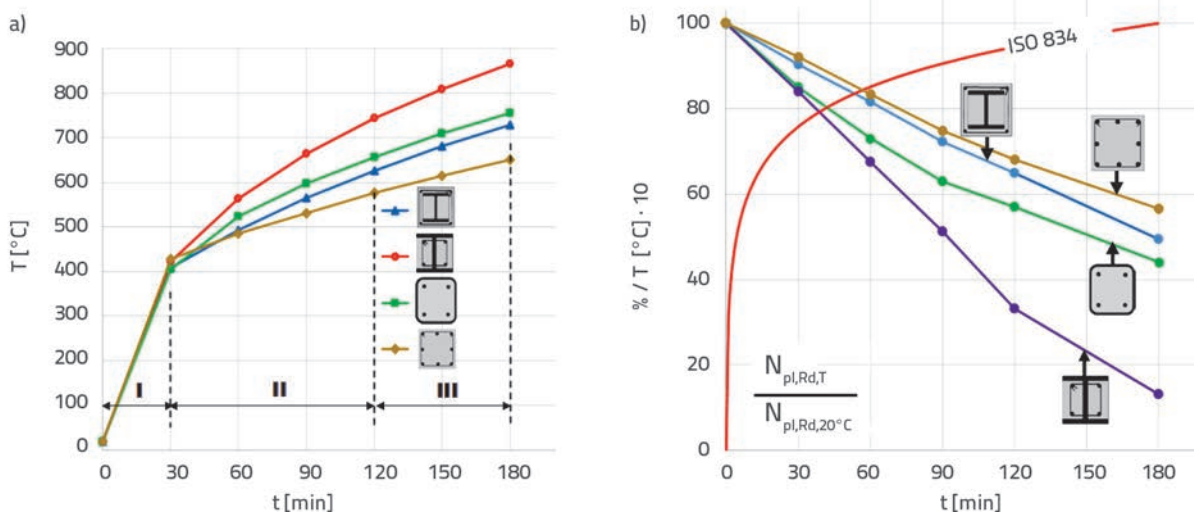


Figure 13. a) Average temperatures in composite column cross sections during fire exposure; b) Axial force bearing capacity of columns for different moments of fire action

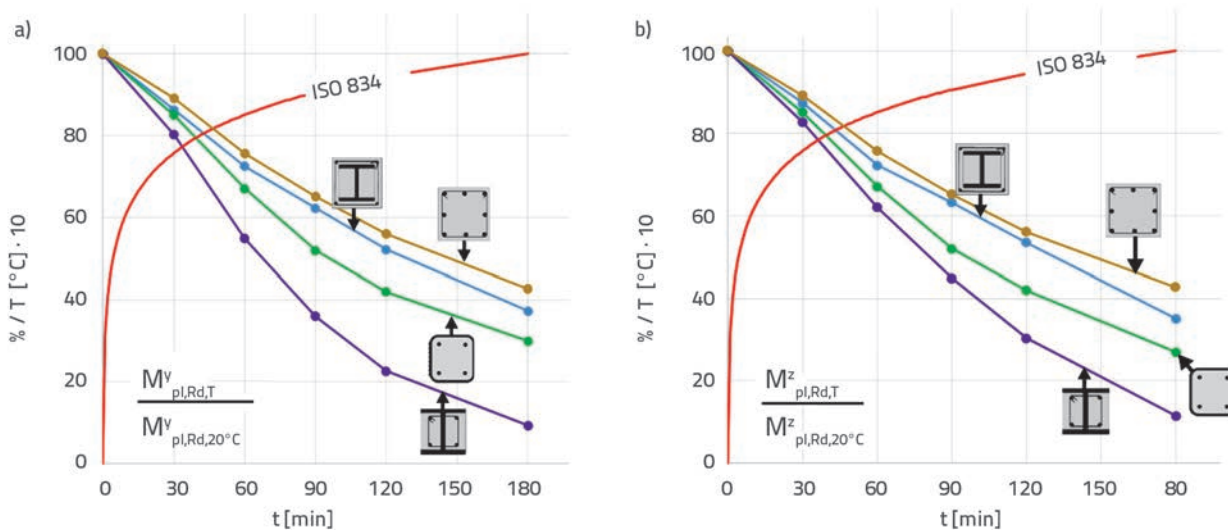


Figure 14. bearing capacity of columns to bending moment about the strong and weak axes, for different moments of fire action

For a defined heating period, the design values of plastic resistances of composite sections to compressive normal force $N_{pl,Rd,T}$ are presented as a percentage of design values of plastic resistance as related to the compressive normal force $N_{pl,Rd,20^{\circ}\text{C}}$ at room temperature, Figure 13.b.

The diagrams in Figure 14 show design values of plastic resistance moments for different types of composite cross sections $M_{pl,Rd,T}$ as a percentage of design values of plastic resistance moments $M_{pl,Rd,20^{\circ}\text{C}}$ at room temperature. The diagrams are produced for the analysed types of composite columns exposed to standard fire according to ISO 834. The left-side diagram shows the bearing capacity for the bending moment about the strong axis, while the right-side diagram shows the bearing capacity for the bending moment about the weak axis of the section.

4. Conclusion

The rise of temperature in the composite column cross sections, as a result of fire action, decreases the bearing capacity of cross sections with regard to the axial compression force and biaxial bending. The reduction in bearing capacity depends on the type of cross section, heating time, fire scenario, etc.

The highest loss of the M – N bearing capacity was observed in the cross sections where the steel profile is directly exposed to heating, as in PES – partially encased sections. A minimum reduction in the M–N bearing capacity was observed in sections where the steel profile is protected with concrete lining (FES section). As concrete is characterized by low thermal conductivity, it prevents rapid penetration of temperature into the steel element and reinforcement thus ensuring better

behaviour of the column (Figure 14). For the same reason, the reinforced concrete column has highest fire resistance and the lowest reduction of bearing capacity.

The lowest decrease of the M-N bearing capacity in case of heating is observed in the FES composite column cross section (Figure 10). The reduction of bearing capacity is almost linear.

As a result of its position in the CFS-concrete filled tubular cross section, the steel profile is directly exposed to fire action, and so high temperatures are reached at the very beginning of the heating process, which is why a significant reduction in the material properties of steel is observed. For that reason, there is a considerable reduction in the M-N interaction curves during the first hour of fire action. With further heating, the temperature slowly penetrates into the concrete core and this effect results in a slow decrease of the remaining M-N bearing capacity of the column.

The difference in the loss of the M-N bearing capacity of the FES and CFS cross sections was not considerable in some heating intervals. The biggest value of 9 % was attained one hour after exposure to fire and this value decreased with further heating. After three hours of heating it dropped down to 3.5 %. This effect must definitely be taken into account when choosing a

proper type of column cross section, especially in the light of considerable advantages of the CFS columns over the PES columns in construction without formwork, simpler connections to the girder elements etc. Also, the possibility for additional fire protection at the perimeter of the CFS columns gives them a considerable advantage over the remaining columns types.

The reduction in the M-N bearing capacity of the PES section in relation to other two analysed sections is 14 % after the first hour of heating, 32 % after two hours of heating, and 36.3 % after three hours of heating. These data indicate that their application in structures that could be exposed to fires is not justified without an additional protection (insulation) of the section.

Average temperature diagrams for analysed types of composite column cross sections, given in Figure 13a, show very clearly the penetration of temperature into the cross section for specific heating intervals. The shapes of the curves are very similar for the diagrams presenting the loss of bearing capacity of cross sections due to axial compressive force (Figure 13b) and the loss of bearing capacity at bending moments about both axes (Figure 14). The results of this investigation confirm the fact that high temperatures caused by fire action decrease the M-N bearing capacity of composite columns.

REFERENCES

- [1] EN 1991-1-2: Eurocode 1: Actions on structures - Part 1-2: General actions - Actions on structures exposed to fire, 2002.
- [2] EN 1992-1-2: Eurocode 2: Design of concrete structures - Part 1-2: General rules. Structural fire design, 2004.
- [3] EN 1994-1-1: Eurocode 4: Design of composite steel and concrete structures - Part 1-1: General rules and rules for buildings, 2004.
- [4] EN 1994-1-2: Eurocode 4: Design of composite steel and concrete structures - Part 1-2: General rules. Structural fire design, 2005.
- [5] Androjić, B., Dujmović, D., Lukačević, I.: Projektiranje spregnutih konstrukcija prema Eurokodu 4, I.A. Projektiranje, Zagreb, 2012.
- [6] Lazarevska, M., Knežević, M., Cvetkovska, M., Ivanišević, N., Samardžioska, T., Trombeva-Gavriloska, T.: Fire resistance prognostic model for reinforced concrete columns, GRAĐEVINAR 64(2012) 7, pp. 565-571.
- [7] Cvetkovska, M., Milanović, M., Jovanoska, M., Cifliganec, C.: Parametric analysis of fire resistance of centrally loaded composite steel-concrete columns, 15th International Symposium of Macedonian Association of Structural Engineers, Ohrid, Makedonija, 2013.
- [8] Milanović, M., Cvetkovska, M.: Zavisnost požarne otpornosti centrično opterećenih spregnutih stubova od dimenzija preseka, Godišnji zbornik GNP 2014, Žabljak, Montenegro, 2014.
- [9] Milanović, M., Filipovski, A., Cvetkovska, M., Cvetanovski, P.: Analiza spregnutih stubova od čelika i betona izloženih požaru, Teorijska i eksperimentalna istraživanja konstrukcija i njihova primena u građevinarstvu, Nacionalni simpozijum sa međunarodnim učesćem, Niš, 2010.
- [10] Caldas, R.B., Sousa Jr, J.B.M., Fakury, R.H.: Interaction diagrams for design of concrete-filled tubular columns under fire, Proceedings of SDSS-Stability and Durability of Steel Structures, Rio de Janeiro, Brazil, 2010.
- [11] Sousa Jr, J.B.M., Caldas, R.B., Fakury, R.H.: Interaction diagrams for concrete-filled tubular sections under fire, Proceedings of Tubular Structures XII (eds. Shen, Z.Y., Chen, Y.Y., Zhao, X.Z.), Taylor & Francis Group, London, 2009
- [12] Fenollosa, E., Cabrera, I.: Analysis of composite section columns under axial compression and biaxial bending moments, Structures and Architecture: Concepts, Applications and Challenges, ISBN 978-0-415-66195-9, Taylor & Francis Group, London, 2013., [http://dx.doi.org/10.1061/\(ASCE\)0733-9445\(2001\)127:6\(678\)](http://dx.doi.org/10.1061/(ASCE)0733-9445(2001)127:6(678))
- [13] Chen, S.F., Teng J.G., Chan, S.L.: Design of bi-axially loaded short composite columns of arbitrary section, Journal of Structural Engineering, ASCE 2001, 127/6, pp. 78-85.
- [14] Cvetkovska, M.: Nonlinear stress strain behavior of RC elements and RC frames exposed to fire, PhD thesis, University "St. Cyril and Methodius", Civil Engineering Faculty-Skopje, 2002.
- [15] SAFIR-Computer program, University of Liege, Belgium, 2014.
- [16] Anderberg, Y., Magnusson, S.E., Pettersson, O., Thelandersson, S., Wickstrom, U.: An analytical approach to fire engineering design of concrete structures, International Symposium on Concrete and Structures. ACI Publications SP-55-16: 409-437, 1986.
- [17] Torić, N., Harapin, A., Boko, I.: Numerical model for determining fire behavior of structures, GRAĐEVINAR 64(2012) 1, pp. 1-13.
- [18] Gillie, M.: The behaviour of steel-framed composite structures in fire, PhD thesis, University of Edinburgh, 2000.
- [19] Adlinge, S.S., Gupta, A.K.: Study of Ultimate Load Capacity of Concrete Encased steel Columns using Finite Element Method, International Journal of Advance Research, IJOAR.org, 2013
- [20] Kuranovas, A., Goode, D., Kazimieras, A.: Load bearing capacity of concrete filled steel columns, Journal of Civil Engineering and Management, Taylor & Francis, pp. 21-33, 2010.